TABLE I. Hospitals That Participated in This Study (GREAT Study: Gunma GIST Research Evaluation Analysis Treatment Study)

Hospital	Number of cases
Gunma Prefectural Cancer Center	62
Gunma University Hospital	42
Saitama Medical Center, Saitama Medical University	32
Gunma Chuo General Hospital	27
Saiseikai Maebashi Hospital	27
Fujioka General Hospital	17
Haramachi Red Cross Hospital	12
Isesaki Municipal Hospital	9
Gunma Prefectural Cardiovascular Center	2
Kiryu Kosei General Hospital	2
Maki Hospital	2
Total	234

findings, were obtained from the patients' surgical records and pathology reports.

Among the 234 patients, the cases of the 41 patients with unresectable or recurrent GIST that were treated with imatinib mesylate were analyzed in detail. Patients in which resection resulted in macroscopic residual lesions (R2 resection) were included in this study, but patients that underwent R0 resection and received adjuvant therapy with imatinib were excluded. Patient data regarding age, sex, tumor location, tumor size, histological status (mitotic count and Ki-67 labeling index), and prognostic outcome were collected from clinical charts. The tumor response was evaluated using computed tomography (CT) or fluorodeoxyglucose positron emission tomography/CT (FDG-PET/CT) every 4–6 months during the imatinib treatment. The tumor response was objectively evaluated by the surgeons or oncologists at each institute according to the guidelines for evaluating the response of solid tumors to treatment [9]. The treatments employed after disease progression were independently chosen by the physicians at each hospital. Various treatments were employed for this purpose, such as surgical intervention, an increased imatinib dose, sunitinib treatment, and best supportive care.

The imatinib treatment response rate, overall survival (OS), progression-free survival (PFS), and the factors affecting prognosis were retrospectively analyzed among the patients with unresectable advanced or recurrent GIST who received imatinib treatment.

Survival curves were calculated according to the Kaplan-Meier method. Survival was defined as the time from the initiation of the first dose of imatinib. The differences between survival curves were examined using the log-rank test. Univariate and multivariate survival analyses were performed using the Cox proportional hazards model.

TABLE II. Characteristics of All 234 GIST Patients

	GIST (n = 234)
Age (years) (mean ± SD)	64.1 ± 11.6
Range	22–87
Gender M/F	129:105
Tumor size (mm) (mean ± SD)	58.0 ± 53.7
Range	2–270
Primary site	n (%)
Stomach	169 (72.2)
Small intestine	35 (15.0)
Duodenum	9 (3.8)
Omentum	6 (2.6)
Colon	6 (2.6)
Rectum	2 (0.9)
Esophagus	2 (0.9)
Others	3 (1.3)

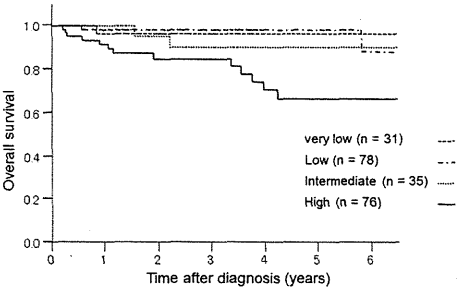

Fig. 1. Overall survival of all 234 GIST patients. While the median follow-up period of the patient population was slightly short (3.2 years), the 3-year survival rate was 92.1%, and even the high risk group exhibited a relatively good 3-year survival rate (84.9%).

P values of less than 0.05 were considered to indicate statistically significant results. All statistical analyses were performed with the JMP 5.0 for Windows software package (SAS Institute Inc., Cary, NC).

RESULTS

Clinicopathological Features and Survival of the 234 Patients

Table II shows the clinicopathological features of all 234 patients. In these patients, the primary lesion was located in the stomach (169 cases; 72.2%), small intestine (35 cases; 15.0%), duodenum (9 cases; 3.8%), or other locations. Of the 234 tumors, it was possible to categorize 220 of them according to the Fletcher classification [10]. Accordingly, 31 (14.1%), 78 (35.5%), 35 (15.9%), and 76 (34.5%) cases were classified as very low risk, low risk, intermediate risk, and high risk (including clinically malignant cases), respectively. Figure 1 shows the OS rate of all 234 patients. While the median follow-up period was slightly short (3.2 years), the 3-year survival rate was 92.1%, and even the high risk group exhibited a relatively good 3-year survival rate (84.9%).

Clinicopathological Features of the 41 Patients With Unresectable or Recurrent Disease Who Received Imatinib Treatment

The clinicopathological features of the 41 patients who received imatinib treatment are shown in Table III. Unresectable advanced GIST was present at the time of diagnosis in 17 cases (41.5%), and the factor responsible for the unresectable nature of the disease was multiple liver metastases in 13 cases and peritoneal dissemination in 6 cases (some cases exhibited both factors). GIST recurred after resection in 24 cases (58.5%). The recurrence took the form of liver metastasis (17 cases), peritoneal dissemination (9 cases), local recurrence (2 cases), lung metastasis (1 case), adrenal metastasis (1 case), or spleen metastasis (1 case, some cases exhibited multiple types of metastasis). The mean tumor size was about 10 cm. As for the location of the primary lesion, the stomach was the most common site (19 cases, 46.3%), followed by the small intestine (14 cases, 34.1%), and the male/female ratio of the 41 patients was markedly higher than that for all 234 patients (1.93 vs. 1.23; Table III).

Overall Response to Imatinib

Seven patients (17.1%) achieved a complete response (CR) according to CT or PET/CT, 20 (48.8%) achieved a partial response

TABLE III. Characteristics of the 41 Patients Who Received Imatinib Treatment

	GIST (n = 41)
Age (years) (mean ± SD)	63.0 ± 13.3
Range	24–83
Gender M/F	27:14
Primary tumor size (mm) (mean ± SD)	100.7 ± 58.8
Range	32–250
Primary site	n (%)
Stomach	19 (46.3)
Small intestine	14 (34.1)
Duodenum	2 (4.9)
Omentum	1 (2.4)
Colon	1 (2.4)
Rectum	1 (2.4)
Esophagus	1 (2.4)
Others	2 (4.9)

(PR), 8 (19.5%) had stable disease (SD), and 6 (14.6%) had progressive disease (PD), yielding a response rate of 65.9% and a disease control rate (CR + PR + SD) of 85.4%. Nine patients received sunitinib treatment as a second-line therapy.

Toxicity of Imatinib

The most common adverse events were edema (58.5%), fatigue (58.5%), skin rash (17.1%), and nausea (12.2%). Most adverse effects were successfully controlled with medication in outpatient clinics. No treatment-related deaths occurred in this study.

Survival Analysis

Figures 2 and 3 show the OS and PFS of the 41 patients that received imatinib treatment. Survival was calculated from the start of imatinib therapy, and the median follow-up period was 4.0 years. Regarding OS, the 1-year, 2-year, and 3-year OS rates were 92.3%, 74.9%, and 53.8%, respectively. The median PFS period was 39.8 months.

Univariate and Multivariate Survival Analyses

Univariate analysis based on the Cox proportional hazards model showed that achieving a good overall response (CR + PR) (RR: 2.00; 95%CI: 1.16–3.45) and imatinib dose reduction (RR: 2.62; 95%CI: 1.42–5.62) were significantly correlated with a good prognosis (Table IV). Tumor size (diameter <10 cm) ($P = 0.072$) and gastric GIST ($P = 0.059$) tended to be associated with better OS, but these associations were not significant. Fletcher risk classification ($P = 0.687$), the site of metastasis ($P = 0.843$), surgical intervention after the detection of disease progression ($P = 0.899$), and the use of sunitinib therapy as a second-line treatment ($P = 0.286$) were not significantly correlated with prognosis.

Multivariate analysis confirmed that achieving a good overall response (CR + PR) (RR: 2.33; 95%CI: 1.29–4.37) and the presence of imatinib dose reduction (RR: 3.05; 95%CI: 1.53–7.18) were independent prognostic factors (Table IV).

Fig. 2. Overall survival of the 41 patients who received imatinib treatment. Survival was calculated from the start of imatinib therapy, and the median follow-up period was 4.0 years. The 1-year, 2-year, and 3-year overall survival rates were 92.3%, 74.9%, and 53.8%, respectively.

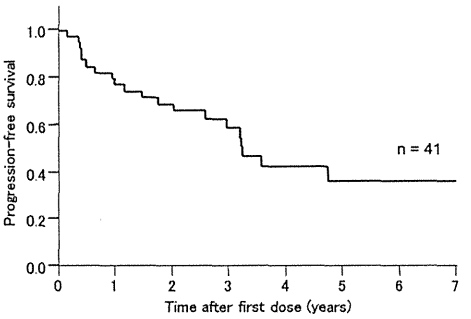

Fig. 3. Progression-free survival of the 41 patients who received imatinib treatment. The median PFS period was 39.8 months.

DISCUSSION

There is limited data available concerning the long-term outcomes of imatinib treatment in Japanese or Asian patients with advanced or recurrent GIST. In this study, we present the results of a Japanese multicenter study of 41 patients with unresectable or recurrent GIST.

There have been two large-scale clinical trials of imatinib treatment for advanced/unresectable GIST. The follow-up data for the patients in the B2222 study, a large scale Phase II study conducted in the USA and Finland, were reported at the 2011 annual meeting of the American Society of Clinical Oncology (ASCO) [4,11,12]. In the latter study, the median follow-up period for patients with unresectable or recurrent GIST who underwent imatinib treatment was 9.4 years [12]. In addition, it was demonstrated that the risk of tumor progression significantly decreased after 6 years of imatinib treatment. Whilst the probability of disease progression was 35–48% for patients that had received fewer than 6 years of imatinib treatment, the probability of disease progression decreased to 5.3% after 6 years of imatinib treatment. As for the other study, the Phase III BFR14 trial performed by the French Sarcoma Group was designed to assess the effect of discontinuing imatinib therapy on patients with advanced GIST. The latter trial was an open-label study in which patients with advanced GIST whose tumors had been controlled (CR, PR, or SD) by imatinib treatment were randomized to the interrupt (I-group) or continue group (C-group) after their disease had been controlled with imatinib treatment for 1, 3, or 5 years. The reports presented by the above group at the 2012 ASCO annual meeting demonstrated that PFS was significantly lower in the I-group than in the C-group. The median PFS periods of the I-group and C-group were as follows: 7 and 29 months in the 1-year study, 9 and 60 months in the 3-year study, and 13 months and not reached in the 5-year study,

TABLE IV. Univariate and Multivariate Analyses (Cox Proportional Hazards Model)

	Univariate analysis		Multivariate analysis	
	RR (95%CI)	*P*-value	RR (95%CI)	*P*-value
Gender (F/M)	1.41 (0.79–2.96)	0.266		
Age (≤60/≥61)	1.08 (0.65–1.84)	0.760		
Overall response (CR + PR/SD + PD)	2.00 (1.16–3.45)	**0.013**	2.33 (1.29–4.37)	**0.005**
Primary tumor size (≤10 cm/>10 cm)	1.64 (0.96–2.97)	0.072		
Risk classification (intermediate/high)	1.14 (0.63–2.39)	0.687		
Primary site (stomach/others)	1.71 (0.98–3.28)	0.059	1.49 (0.85–2.89)	0.17
Metastatic site (liver/peritoneum)	1.06 (0.55–1.89)	0.843		
Imatinibdose reduction (present/absent)	2.62 (1.42–5.62)	**0.0014**	3.05 (1.53–7.18)	**0.001**
Surgical intervention (present/absent)	1.03 (0.60–1.78)	0.899		
Second-line sunitinib treatment (absent/present)	1.36 (0.76–2.32)	0.286		

RR, relative risk; CI, confidence interval. Bold type; $P < 0.05$.

respectively. The 1-year PFS rates of the I-group and C-group were as follows: 31% and 85% in the 1-year study, 32% and 92% months in the 3-year study, and 71% and 92% in the 5-year study, respectively [13–16] (Table V). These results showed that rapid disease progression occurs if imatinib is interrupted in GIST patients whose tumors are controlled by long-term imatinib treatment. The results of these two large-scale, long-term trials demonstrate that the risk of tumor progression decreases with increased treatment duration. Furthermore, the interruption of imatinib treatment in responsive and controlled patients results in a high risk of disease progression. On the basis of this evidence, the GIST clinical guidelines in various countries recommend that imatinib treatment for patients with advanced GIST should be continued until the tumor progresses [17–19].

In Japanese patients, whose body weight is lower than that of Western patients, it is recommended that imatinib treatment should start at a dose of 400 mg per day [20]. Continuous imatinib dosing is important for the management of advanced GIST. In our study, there were 19 patients (46.3%) who had their imatinib dose reduced to 300 mg or 200 mg per day during long-term treatment. The reasons why the patients had imatinib dose reduced were adverse events and financial reasons. The most common adverse events were edema (grade 2: 63.2%), fatigue (grade 2: 52.6%), skin rash (grade 2: 21.1%), and diarrhea (grade 2: 15.8%) in 19 patients (those with duplication). In this study, although there was exception, imatinib dose reduction was performed when PR and SD followed a long period at least one year, and low dose imatinib treatment was continued without interruption. Once disease showed progression, imatinib dose escalation to 400 mg/day was done. Demetri et al. reported that it is important to maintain a sufficient plasma imatinib level in order to achieve and maintain a clinical response in patients with GIST [21]. Although nearly 50% of our patients required imatinib dose reduction, the median PFS period was 39 months, which was longer than the median PFS period of 24 months observed in the B2222 study. Furthermore, univariate and multivariate analyses based on the Cox proportional hazards model showed that imatinib dose reduction was significantly correlated with a good prognosis. We cannot explain the reason for this at present, but the following explanations are suggested. First, most of the patients in the imatinib dose reduction group (15 out of 19 cases) achieved a good response (CR or PR), whereas the non-responders experienced rapid disease progression and had to stop receiving imatinib therapy early; i.e., before they could undergo imatinib dose reduction. Secondly, the patients who experienced imatinib dose reduction were treated without interruption for longer than those in the standard dose group; i.e., the median imatinib administration period was 41.5 months among the patients who experienced dose reduction (19 cases) and 19.6 months among the patients who did not undergo imatinib dose reduction (22 cases). All except two of the patients who experienced dose reduction continued to receive imatinib treatment until their disease progressed. As Japanese patients tend to have small statures than Western patients, their imatinib plasma levels might remain at effective concentrations even after dose reduction. Thus, further studies involving the measurement of plasma imatinib levels are required. Tumor size (diameter <10 cm) tended to be associated with better OS, but not significant ($P = 0.072$). Fletcher risk classification was not significantly correlated with prognosis ($P = 0.687$). Risk classifications including tumor size predict a risk of recurrence, they may not reflect the outcome of imatinib treatment.

TABLE V. Summary of BFR14 Trial

	One-year PFS rate
After the treatment of controlled disease for1 year	I-group: 31% C-group: 85%
After the treatment of controlled disease for 3 years	I-group: 32% C-group: 92%
After the treatment of controlled disease for 5 years	I-group: 71% C-group: 92%

PFS, progression-free survival.

Although we do not recommend imatinib dose reduction for Japanese GIST patients, our results suggest that it is reasonable to determine the maintenance dose of imatinib for each patient on the basis of assessments of adverse effects, age, and body weight.

In conclusion, long-term imatinib therapy is recommended for patients with non-progressive disease. If patients experience significant toxicities, temporary imatinib dose reduction and treatment continuation might be a useful strategy.

REFERENCES

1. Hirota S, Isozaki K, Moriyama Y, et al.: Gain-of-function mutation of c-kit in human gastrointestinal stromal tumors. Science 1998;279:577–580.
2. Kindblom LG, Remotti HE, Aldenborg F, et al.: Gastrointestinal pacemaker cell tumor (GIPACT). Gastrointestinal stromal tumors show phenotypic characteristics of the intestinal cells of Cajal. Am J Pathol 1998;152:1259–1269.
3. Heinrich MC, Corless CL, Duensing A, et al.: PDGFRA activating mutation in gastrointestinal stromal tumors. Science 2003;299:708–711.
4. Demetri GD, von Mehren M, Blanke CD, et al.: Efficacy and safety of imatinib mesylate in advanced gastrointestinal stromal tumors. N Engl J Med 2002;347:472–480.
5. Kanda T, Ishikawa T, Hirota S, et al.: Prospective observational study of imatinib therapy in Japanese patients with advanced

gastrointestinal stromal tumors: Long-term follow-up and second malignancy. Jpn J Clin Oncol 2012;42:578–585.
6. Saito S, Nakata K, Kajiura S, et al.: Long-term follow-up outcome of imatinib mesylate treatment for recurrent and unresectable gastrointestinal stromal tumors. Digestion 2013;87:47–52.
7. Nilsson B, Bumming P, Meis-Kindblom JM, et al.: Gastrointestinal stromal tumors: The incidence, prevalence, clinical course, and prognostication in the preimatinib mesylate era – a population-based study in western Sweden. Cancer 2005;103:821–829.
8. Tryggvason G, Gislason HG, Magnusson MK, et al.: Gastrointestinal stromal tumors in Iceland, 1990–2003: The Icelandic gist study, a population-based incidence and pathologic risk stratification study. Int J Cancer 2005;117:289–293.
9. Therasse P, Arbuck SG, Eisenhauer EA, et al.: New guidelines to evaluate the response to treatment in solid tumors, European Organization for Research and Treatment of Cancer, National Cancer Institute of the United States, National Cancer Institute of Canada. J Natl Cancer Inst 2000;92:205–216.
10. Fletcher CD, Berman JJ, Corless C, et al.: Diagnosis of gastrointestinal stromal tumors: A consensus approach. Hum Pathol 2002;33:459–465.
11. Blanke CD, Demetri GD, von Mehren M, et al.: Long-term results from a randomized phase II trial of standard- versus higher-dose imatinib mesylate for patients with unresectable or metastatic gastrointestinal stromal tumors expressing KIT. J Clin Oncol 2008;26:620–625.
12. von Mehren M, Heinrich MC, Joensuu H, et al.: Follow-up results after 9 years of the ongoing, phase II B2222 trial of imatinib mesylate in patients with metastatic or unresectable KIT+ gastrointestinal tumors (GIST). J Clin Oncol 2011;29:Abstract 10016.
13. Blay JY, Le Cesne A, Ray-Coquard I, et al.: Prospective multicentric randomized phase III study of imatinib in patients with advanced gastrointestinal stromal tumors comparing interruption versus continuation of treatment beyond 1 year: The French Sarcoma Group. J Clin Oncol 2007;25:1107–1113.
14. Le Cesne A, Ray-Coquard I, Bui BN, et al.: Discontinuation of imatinib in patients with advanced gastrointestinal stromal tumours after 3 years of treatment: An open-label multicentre randomised phase 3 trial. Lancet Oncol 2010;11:942–949.
15. Ray-Coquard IL, Bin Bui N, Adenis A, et al.: Risk of relapse with imatinib (IM) discontinuation at 5 years in advanced GIST patients: Results of the prospective BFR14 randomized phase III study comparing interruption versus continuation of IM at 5 years of treatment: a French Sarcoma Group Study. J Clin Oncol (Meeting Abstracts) 2010;28:Abstract 10032.
16. Bertucci F, Ray-Coquard I, Bui Nguyen B, et al.: Effect of five years of imatinib on cure for patients with advanced GIST: Updated survival results from the prospective randomized Phase III BFR14 trial. J Clin Oncol 2012;30:Abstract 10095.
17. Demetri GD, von Mehren M, Antonescu CR, et al.: NCCN task force report: Update on the management of patients with gastrointestinal stromal tumors. J Natl Compr Canc Netw 2010;8: S1–41.
18. Casali PG, Blay JY: Gastrointestinal stromal tumors: ESMO clinical practice guidelines for diagnosis, treatment and follow-up. Ann Oncol 21:v98–102.2010.
19. Kubota T: Gastrointestinal stromal tumor (GIST) and imatinib. Int J Clin Oncol 2006;11:184–189.
20. Nishida T, Shirao K, Sawaki A, et al.: Efficacy and safety profile of imatinib mesylate (STI571) in Japanese patients with advanced gastrointestinal stromal tumors: A phase II study (STI571B1202). Int J Clin Oncol 2008;13:244–251.
21. Demetri CD, Wang Y, Wehrle E, et al.: Imatinib plasma levels are correlated with clinical benefit in patients with unresectable/ metastatic gastrointestinal stromal tumors. J Clin Oncol 2009;27: 3141–3147.

J Hepatobiliary Pancreat Sci (2014) 21:856–863
DOI: 10.1002/jhbp.144

ORIGINAL ARTICLE

Reconfirmation of the anatomy of the left triangular ligament and the appendix fibrosa hepatis in human livers, and its implication in abdominal surgery

Kimitaka Kogure · Itaru Kojima · Hiroyuki Kuwano · Toshiyuki Matsuzaki · Hiroshi Yorifuji · Kuniaki Takata · Masatoshi Makuuchi

Published online: 20 August 2014

Abstract
Background The aim of the present study was to clarify the anatomy between the left triangular ligament (LTL) and the appendix fibrosa hepatis (AFH) in order not to sever the AFH when dissecting the LTL.
Methods Totals of 43 and 27 cadaveric livers were examined macroscopically and histologically, respectively.
Results The LTL attached itself to the diaphragmatic surface of the AFH through almost all lengths of the AFH. This might be the reason why AFH is so often dissected together with the LTL. There were two types of relation between the LTL and the AFH; in one type, the starting point of the LTL existed on the left liver and in the other type, it was on the AFH. Twenty-five of 27 AFH included remnants of the bile duct and 12 of 25 AFH had comparatively large bile ducts, which was unexceptionally accompanied by the well-developed peribiliary vascular plexus. AFH showed a variety of shapes, such as rectangular (6/43), long triangular (4/43), short triangular (7/43), triangular plus cordlike (11/43), cordlike (12/43) and bifurcated (3/43) types.
Conclusions As AFH sometimes includes relatively large bile ducts, it is recommended for surgeons to sever the AFH not just simply by electrocautery but by ligating its stump securely.

Keywords Appendix fibrosa hepatis · Human liver

K. Kogure (✉) · I. Kojima
Laboratory of Cell Physiology, Institute for Molecular and Cellular Regulation, Gunma University, 3-39-15 Showamachi, Maebashi, Gunma 371-8512, Japan
e-mail: kogurefm@oak.gunma-u.ac.jp

H. Kuwano
Department of General Surgical Science, Graduate School of Medicine, Gunma University, Maebashi, Gunma, Japan

T. Matsuzaki
Department of Anatomy and Cell Biology, Graduate School of Medicine, Gunma University, Maebashi, Gunma, Japan

H. Yorifuji
Department of Neuromuscular and Developmental Anatomy, Graduate School of Medicine, Gunma University, Maebashi, Gunma, Japan

K. Takata
Office of the President, Gunma University, Maebashi, Gunma, Japan

M. Makuuchi
Department of Surgery, Japanese Red Cross Medical Center, Shibuya, Tokyo, Japan

Introduction

Appendix fibrosa hepatis (AFH) is an atrophied hepatic tissue protruding from the left external edge of the left liver [1–4]. Regardless of various shapes, most AFHs contain remnants of hepatic tissue; namely portal vein (PV), hepatic artery (HA), bile duct (BD), hepatic vein (HV) and sometimes degenerative liver cell cord [5–8]. Consequently, severing the AFH without ligation has a risk of postoperative bile leakage, from which bile peritonitis occasionally results. Many surgeons might have experienced the bile leakage from the stump of the AFH after the dissection of the left triangular ligament (LTL) around the esophagogastric junction, especially in the total gastrectomy [9–12]. It was caused by the fact that the AFH was severed simultaneously though only LTL was targeted for the dissection. And it may result from the difficulty in distinguishing the AFH from the LTL when viewed from the diaphragmatic side. The LTL itself exists between the AFH and the diaphragm, and tightly connects them through almost the entire length of the AFH. Therefore, a considerable area of the

diaphragmatic surface of the AFH is hidden by the LTL. To avoid the inadvertent dissection of the AFH, reconfirmation of the anatomy between the AFH and the LTL must be required.

In the present study we intended to clarify the real anatomical relation between the AFH and the LTL to inquire into the reason why AFH and LTL are at times confused with each other and inadvertently dissected together. Also we intended to clarify the reason why postoperative bile leakage occurs from the bile ducts remaining in the AFH, in spite of the atrophied hepatic tissue.

Materials and methods

Livers were extirpated with AFH, LTL and the diaphragm in a mass from 43 adult cadavers (23 male, 20 female, mean age 84.0 ± 1.3) provided by the Department of Anatomy, Gunma University, Graduate School of Medicine, Maebashi, Japan.

Ligaments (i.e. right triangular, coronary, left triangular, falciform, round, hepatoduodenal, hepatogastric and hepatorenal ligaments) fixing the liver to the diaphragm or the abdominal wall were carefully inspected from diaphragmatic and visceral sides. Then, the shape of the AFH was examined macroscopically and it was classified into six types according to the classification of Gao and Roberts, that is, rectangular, triangular (short and long), triangular plus cordlike, cordlike and bifurcated types [8]. In our study, the triangular type was subdivided into short (<3 cm) and long (>3 cm) triangular types according to the length of the AFH. After that, the interrelation among the left liver, the LTL, the AFH and the diaphragm was macroscopically examined. Then, the diaphragm was removed in a meticulous manner in order not to injure the AFH and the LTL, and the pattern of the bare area that was located between the superior and the inferior layers of the coronary ligament was examined. After the macroscopic observation, the AFH and the LTL including the extremity of the left liver were taken together from 27 cadaveric livers of good condition (14 male, 13 female, mean age 85.1 ± 1.6). These specimens, fixed in 10% formalin solution and preserved in 5% formalin solution, were embedded in paraplast (Oxford Co., St Louis, MO, USA), and sliced into 10-μm-thick sections. The transverse sections containing a part of the left liver, the LTL, the remnant of LTL and the AFH were stained with hematoxylin and eosin and Elastica van-Gieson stain, and the relation among these structures were microscopically investigated. The PV, HA, BD and the remnant of the liver cells and the nerve bundles, were examined for the specimens obtained from the proximal (medial), central and distal (left lateral) one-third regions of the AFH, respectively. Characteristic features of the intrahepatic BD ramifying in the AFH were investigated specifically from the point of view of the postoperative bile leakage. Existence of the peribiliary vascular plexus (PVP), a primary feeding vessel of the intrahepatic bile ducts, was inquired in each BD of the AFH [13–16]. In this study, BD of which diameter is larger than that of adjacent PV was defined as "a relatively large BD", because the diameter of the intrahepatic BD of the normal liver was smaller than that of the adjacent PV in general. The HV of the AFH was excluded from the subject of investigation, because of the difficulty in defining it.

We defined the ligaments of the liver by the definition of Rohen et al. [17] and have adapted Couinaud's segmentation for the nomenclature of the liver [18]. Anatomical consent was obtained from all donors in the form of living will.

Results

Appearance of the AFH *in situ*

Appendix fibrosa hepatis was a fibrous band continuously extending from the left extremity of the left liver to the posterolateral portion of the diaphragm. Various kinds of shapes were found in the AFH. However, regardless of shape, the external appearance of the AFH varied depending on the position from which it was observed. As shown in Figure 1a, it was difficult to see the whole shape of the AFH when looking at it from diaphragmatic side, whereas when it was viewed from the visceral side by temporarily holding the left liver up, its shape was completely identified (Fig. 1b). It was caused by the fact that the LTL of the left liver continuously stretching to the diaphragmatic surface of the AFH or the thick areolar tissue developing under the diaphragmatic sided capsule of the AFH disturbed the observation of the precise shape of the AFH, respectively. Moreover, it was difficult to identify each boundary between them because AFH, LTL and the diaphragm were continuously covered with the same peritoneum. To the contrary, the whole shape of the AFH was clearly observed from the visceral side because there was no tissue that disturbed the observation of the visceral surface of the AFH. Moreover, it was possible to see several vessels that derived from the left liver branching off into the AFH when viewing it from the visceral side. The histology of this case showed that a thick areolar tissue developing under the diaphragmatic-sided capsule of the AFH disturbed the observation of the precise shape of the AFH including the remnants of the liver (figure not shown).

Two types of bare area or two types of the relation between the LTL and the AFH

To perform the safe dissection around the esophagogastric junction it is important to understand the precise relation among the left liver, the LTL and the AFH. Figure 2a shows

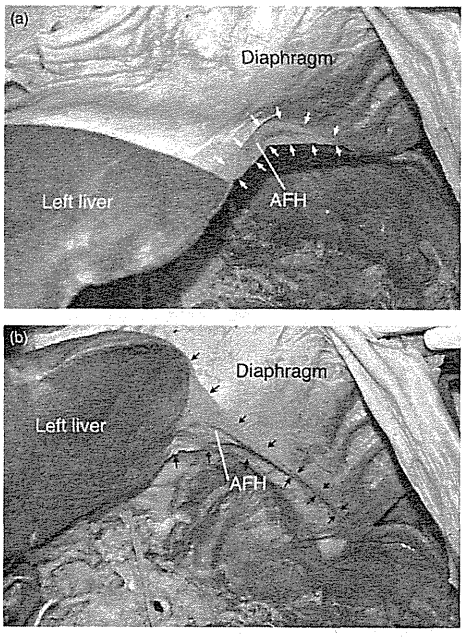

Fig. 1 The appendix fibrosa hepatis (AFH) *in situ*. (**a**) The AFH viewed from the diaphragmatic side. As a thick areolar tissue covered most of the diaphragmatic surface of the AFH only a part of the AFH (the area surrounded by white arrows) can be observed. The under row of the arrows indicates the anterior edge of the AFH. In the upper row the part between the right-sided first arrow and the fourth arrow indicates the pleat of the capsule of the AFH formed by the thick areolar tissue, and the arrows from the fifth to the sixth indicate the reflection of the peritoneum of the AFH. (**b**) The AFH viewed from the visceral side. Whole configuration of the AFH can be seen from the visceral side. Black arrows indicate the anterior and posterior edges of the AFH.

the cut surface of the LTL and the left liver. As shown in Figure 2a, the liver surface facing free peritoneal cavity was covered with two layers of connective tissue. The inner layer enclosing the liver parenchyma was the thin fibrous connective tissue (Glisson's capsule), comparatively rich in elastic fibers, whereas the outer layer was the visceral peritoneum consisting of mono-layer of mesothelium lined by the fibrous connective tissues, which was comparatively rich in collagen fibers. Two layers were not distinguishable in the normal surface of the liver, but they were clearly divided into visceral peritoneum and Glisson's capsule as they approach the peritoneal reflection where the formation of the LTL starts. After the reflection, visceral peritoneum of the left liver became thicker and formed the anterior and posterior layers of the LTL, whereas Glisson's capsule kept surrounding the liver parenchyma in the bare area. The narrow spaces between the anterior and posterior layers of the LTL were filled with areolar tissue, which was continuous with that of the bare area of the left liver. The observation described above is important to better understand the relation between the AFH and the LTL.

Figure 2b,c show two types of the bare area or two types of the relation between the LTL and the AFH. As shown in Figure 2b,c, the two (anterior and posterior) layers of the LTL were continuous with the superior and the inferior layers of the coronary ligament, respectively. The area enclosed with the two layers of the coronary ligament was devoid of the peritoneal covering, and this non-peritoneal surface constituted the "bare area" of the liver. Therefore, the left limit constituted by joining two layers of the coronary ligament corresponded to the left end of the bare area or the beginning (the right extremity) of the LTL.

Two types were recognized on the relations between the LTL and the AFH. In one type, the left limit of the bare area or the beginning (the right extremity) of the LTL existed on the left liver (Fig. 2b). In this type, the LTL was constituted from the reflection of the peritoneum of both left liver and the AFH and the relationship observed between the LTL and the AFH was almost the same as that between the LTL and the left liver, that was shown in Figure 2a. In another type, the bare area extended into the AFH. In this type, the left limit of the bare area or the beginning (the right extremity) of the LTL existed on the AFH; therefore, the LTL was constituted from the reflection of the peritoneum of the AFH (Fig. 2c). In this type, as the bare area extended from the left liver to the AFH, two layers reflecting from the upper surface of the AFH corresponded to the superior and the inferior layers of the coronary ligament of the left liver. The space between two layers was filled with the areolar tissue, which was continuous with that of the bare area of the left liver. There was a similar relationship observed between the coronary ligament and the left liver. In the latter type, the considerable area of the diaphragmatic surface of the AFH was adhered to the diaphragm through the areolar tissue of the bare area; therefore, it was difficult to see the whole shape of the AFH from the diaphragmatic side. The former type was observed in 36 of 43 (84%) cases, and the latter type, in seven cases.

The relations between the LTL and the left liver or between the coronary ligament and the left liver were basically kept as the relations between the LTL and the AFH or between the coronary ligament and the AFH.

Shape of the AFH

The real shape of the AFH could be confirmed only after the diaphragm was stripped from the liver and the AFH. Various shapes ranging from membranous to cord-like types were observed. The shape was classified into six types, namely

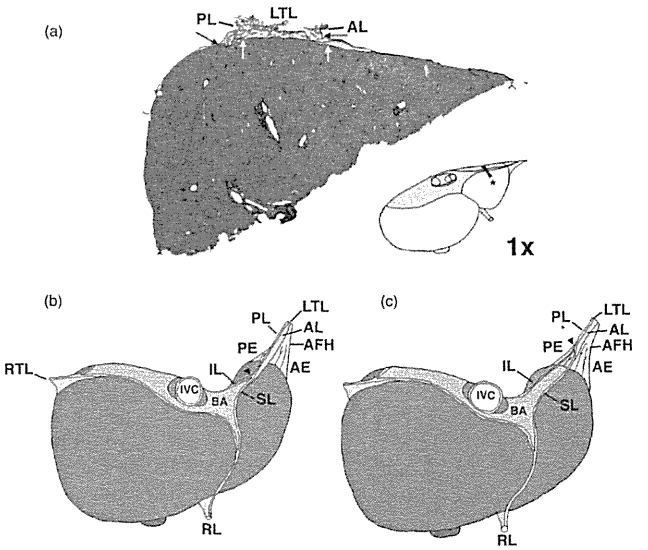

Fig. 2 Cut surface of the left triangular ligament (LTL) on the left liver and two types of the bare area or two types of the relation between the LTL and the appendix fibrosa hepatis (AFH). (**a**) Reflections of the peritoneum surrounding the left liver make up the anterior and posterior layers of the LTL. The portions of the peritoneal reflection making up the posterior and anterior layers of the LTL. Areolar tissue is developed between both layers. HE 1×. * indicates the portion from which the specimen was obtained. Elastica van-Gieson, 40×. (**b**) The bare area of which the left limit exists within the left liver. The superior and inferior layers of the coronary ligament are constituted from the peritoneal reflection of the left liver. The LTL is composed of the reflection of the peritoneum of the left liver and the AFH. (**c**) The bare area of which the left limit exists not on the left liver but on the AFH. A part of the coronary ligaments and the LTL exist together on the AFH. The superior and inferior layers of the coronary ligament are composed of the peritoneal reflection of the left liver and the AFH. The LTL is composed of the reflection of the peritoneum of the AFH. Black arrows (**a**): the portions of the peritoneal reflection, White arrows (**a**): Glisson's capsule surrounding the left liver, arrow heads (**b** and **c**): the left limit of the bare area or the right extremity of the LTL. *AL* and *PL* anterior and posterior layers of the LTL, *SL* and *IL* superior and inferior layers of the coronary ligament, *AE* and *PE* anterior and posterior edges of the AFH, *BA* bare area, *IVC* inferior vena cava, *RL* round ligament, *RTL* right triangular ligament.

rectangular type (Fig. 3a, 6/43), long triangular type (Fig. 3b, 4/43), short triangular type (Fig. 3c, 7/43), triangular plus cordlike type (Fig. 3d, 11/43), cordlike type (Fig. 3e, 12/43) and bifurcated type (Fig. 3f, 3/43). The mean length of the AFH with standard error was 5.9 ± 0.43 cm (range; 1.5–11.0 cm) and the width of the proximal (medial) side was 2.5 ± 0.3 cm (range; 0.7–11 cm).

Remnants of hepatic tissue in the AFH

Since the AFH is formed by the atrophy of the left liver, the same tissues (PV, HA, BD, HV, liver cells, vagal nerve and lymphatic vessel) constituting the normal liver were found in the AFH (Fig. 4). As shown in Figure 4a,b, in the proximal (medial) region of the AFH, PV, HA and BD did not exist solitarily but as a set in the degenerated portal tract with a denatured (usually flattened) form; however, the complete portal tract including PV, HA and BD decreased in number with going to the distal (left lateral) region. As shown in Table 1, the complete portal tract was observed in 25 of 27 cases in the proximal (medial) one-third region of the AFH, in 18 of 27 cases in the central one-third region of the AFH and in 11 of 27 cases in the distal (left lateral) one-third region of the AFH, respectively. There were cases that lost the BD from the portal tract; however, the PV and the HA remained in the degenerated portal tract as a set. These incomplete portal tracts increased in their number with going to the distal (left lateral) region (two in proximal [medial] region, seven in central region and 14 in distal [left lateral] region, respectively) (Table 1). Remnants of the portal tract of the AFH were basically continuous to those of segment 2 of the left liver. Remnants of liver cells scattered around these portal tracts were observed in 23 of 27 cases in the proximal (medial) one-third region of the AFH, in seven of 27 cases in the central one-third region of the AFH and in one of 27 cases in the distal (left lateral) one-third region of

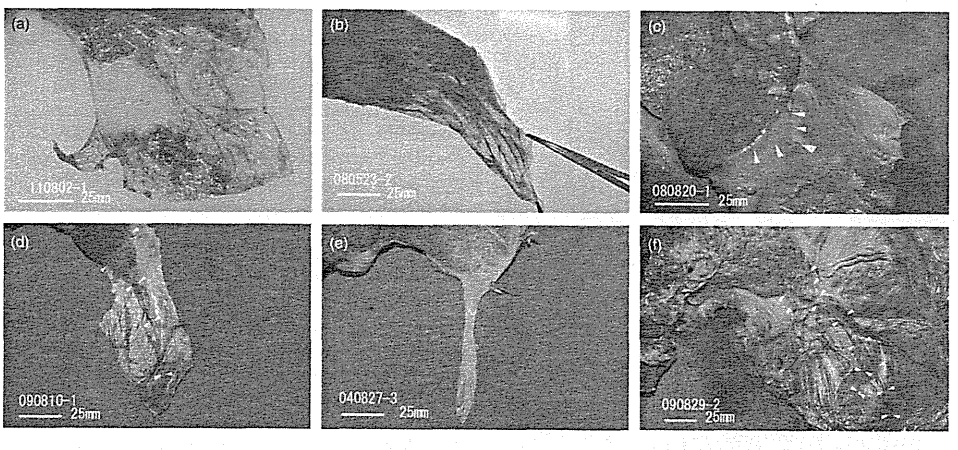

Fig. 3 Six types of the shape in the appendix fibrosa hepatis (AFH). (**a**) Rectangular type, (**b**) long triangular type (>3 cm), (**c**) short triangular type (<3 cm), (**d**) triangular plus cordlike type, (**e**) cordlike type, (**f**) bifurcated type (Distal [left lateral] side is divided into two tails). White arrowheads indicate the margin of each AFH adhering to the diaphragm.

the AFH, respectively. Remnants of nerve fiber were found in 19 of 27 in the all areas of the AFHs (70.3%).

Comparatively large bile ducts and the PVP in the AFH

Among the specimens of the AFH examined microscopically the comparatively large BDs lined with monolayer of cuboidal-columnar epithelium were found in 12 of 25 cases in which remnants of BD remained (48%). In the cases having comparatively large BDs, the PVP, which consisted of micro blood vessels, invariably developed around them (Fig. 4b), whereas in the remaining 13 cases, which portal tract of the AFH had a normal BD in size, no definite development of the PVP was identified around them as shown in Figure 4a. The figure indicating the developed PVP is not shown.

Discussion

Rapant and Hromada [9] quoted an article of Engel [19] and reported 10 portions where remnants of the hepatic tissue with BD remained in the adult liver. Afterward Champeitier [7] also indicated a similar 10 portions including remnants of the BD in the adult liver. The portions indicated by theses predecessor's studies are: (1) appendix fibrosa hepatis; (2) suspensory apparatus of the liver including right triangular ligament (RTL), left triangular ligament and falciform ligament (FL); (3) gallbladder fossa; (4) duodenal impression on liver; (5) esophageal impression on liver; (6) hepatic parenchymal bridge on the round ligament at umbilical fissure; (7) porta hepatis; (8) hepatogastric ligament; (9) inferior vena cava ligament (IVC ligament); and (10) paracaval portion of the caudate lobe which is continuous with the IVC ligament.

These portions except RTL, LTL, FL and hepatogastric ligament are mainly composed of atrophied hepatic tissues including remnants of the PV, HA, BD, nerve fiber and the liver cells [20]. These atrophied hepatic tissues may be formed during the process of the developmental diminution of the fetal liver to adapt its shape to the abdominal cavity as keeping the harmony with other abdominal organs. Therefore, it is quite natural that the remnants of the hepatic tissue which used to exist in the corresponding portions of the fetal liver are found in these atrophied portions of the adult liver. Among those AFH is the biggest one in which remnants of hepatic tissue are found at high rates.

Appendix fibrosa hepatis attaches itself to the extremity of the adult left liver without exception, therefore it is named "appendix fibrosa hepatis or fibrous appendix of liver", but it has not been found in the fetal liver or the neonatal liver at all. Toldt and Zuckerkandl illustrated, in their treatise, a 3-week-old neonate liver without AFH, a 3-month-old infant liver without AFH, a 2-year-old child liver without AFH [1]. Healey and Sterling studied the segmental anatomy of the liver by using 20 fetal and infantile liver casts in order to ascertain any differences between these livers and adult livers; however, any AFH was not found in these liver casts [21]. Gao and Roberts could not find any AFH in the livers of 30 Chinese newborn cadavers [8]. El Gharbawy et al. could find neither AFH nor other atrophied tissues in 10 stillborn baby livers [22]. These observations described above will indicate that the AFH is yet to be

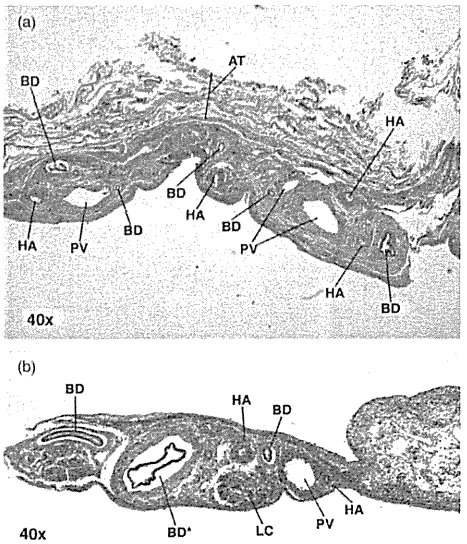

Fig. 4 (**a**) Cut surface of the appendix fibrosa hepatis (AFH) that includes the remnants of the portal tracts similar to those of the normal liver. Portal vein (PV), hepatic artery (HA) and bile duct (BD) exist in the AFH as a set. The diameter of BDs is smaller than that of the neighboring PVs. No definite peribiliary vascular plexus develops around them. HE 40×. (**b**) Cut surface of the AFH that includes relatively large bile ducts (BD*) when these are compared with the neighboring PV. PV, HA and BD exist as a set. Peribiliary vascular plexus developed around the relatively large bile duct. HE 40×. *AT* areolar tissue of the bare area through which the AFH adheres to the diaphragm, *BD* bile duct (wall), *LC* liver cell, *EP* epithelium of the BD. Epithelium is exfoliated from the bile duct wall by artifact

Table 1 Distribution of portal vein (PV), hepatic artery (HA), bile duct (BD) and liver cell (LC) in the appendix fibrosa hepatis (AFH) (total 27 cases)

	Proximal 1/3	Central 1/3	Distal 1/3
Complete portal tract (PV+HA+BD) with LC	23	7	1
Complete portal tract (PV+HA+BD) without LC	2	11	10
Incomplete portal tract (PV+HA)	2	7	14
Not examined	0	2	2
Total	27	27	27

Proximal (medial), distal (left lateral).

formed in the livers of the newborn baby. When is the AFH formed? The figures of the liver illustrated by Toldt and Zuckerkandl may give an important suggestion for the question [1]. In their treatise, a typical AFH was illustrated in the figure of the liver of 4-year-old child and it may suggest that the AFH is formed at least before the fourth year after the birth. It is well known that from the third month of intrauterine life the left liver undergoes a process of atrophy so that at birth the left is smaller in thickness than the right though the left liver is nearly as large as the right liver when viewed from the abdominal side [23, 24]. The observations described above will suggest that the process of the atrophy of the left liver is accelerated after the birth and as the result the AFH is formed during childhood. While the shape of the adult liver is completed, other portions such as gallbladder bed or IVC ligament may also atrophy in the same way as AFH. However, through meticulous review of the literature, no report referring to the correct time when the atrophy of these portions is finished has been found.

Our study showed that the LTL attached itself to the diaphragmatic surface of the left liver and the AFH (Fig. 2). When is the LTL formed? Toldt and Zuackerkndl illustrated a typical LTL in a 3-week-old neonate liver, a 3-month-old infant liver and 2-year-old young child liver, respectively [1]. However, these livers had no AFH in the tip of the left liver. Their observation will suggest that the LTL is already formed on the left liver during the fetal period though the AFH is yet to be formed. However, both LTL and AFH were clearly illustrated in one more figure of 4-year-old child liver by Toldt and Zuackerkndl [1]. The observation will indicate that the LTL of the newborn liver atrophies together with the left liver and that as the result the LTL remains on the diaphragmatic surface of the AFH. This positional relationship between the LTL and the AFH will explain why AFH is so often confused with the free edge of the LTL and is inadvertently severed during the dissection around the esophago-gastric junction [9–12]. As shown in Figure 1b, we, however, showed that the whole configuration of the AFH can be clearly identified when viewing it from the visceral side. Therefore, looking over the visceral surface of the AFH by lifting up the left liver will be a key manipulation not to fail to notice the AFH including the remnants of BD. It is necessary to have this in mind when dissecting the LTL on the diaphragm.

Our study showed that there were two types of bare area. In one type its left limit existed within the left liver, whereas in the other type on the AFH. The reason why such different types of bare area are formed may depend on the extent of the atrophy of the left liver. In the latter type it becomes more difficult to distinguish the LTL from the AFH.

Appendix fibrosa hepatis generally includes remnants of PV, HA, BD and liver cell cords. The degeneration of these remnants (especially liver cell cord and the BD) becomes more prominent going to the tip of the AFH. This means that the atrophy, at first, starts from the left tip of the left liver and goes toward the central portion of the left liver. The transverse section of the portal tract observed in the normal liver is usually round or oval, whereas in the AFH it was

generally flat, as shown in Figure 4a,b. This is probably attributable to the membranous atrophy of the left liver.

The postoperative bile leakage will happen as a result of an inadvertent severing of the BDs persisting within the AFH. This indicates that a considerably larger bile channel exists between the left liver and the AFH. Healey and Schroy injected vinyl acetate into the common bile ducts of 100 cadaveric livers and found that the BD of segment 2 begins at the upper outer angle of the liver and at times (5%) extends into the AFH as a vas aberrans hepatis [25]. Foster injected the same material into the common bile duct and observed the grossly visible BDs in the AFH in three of nine livers [6]. Kekis et al. made liver casts of 80 cadaveric livers in the same way and found the BDs branching into the LTL (AFH) in 13 (16%) of these cases [12]. They also observed the bile staining in 15 of 134 cases (11%) on the gauze swab, which was placed on the region where the LTL was dissected without ligation. These reports described above will indicate that there is a large bile duct channel between the left liver and the AFH and that it may cause postoperative bile leakage in a certain ratio.

Our histological examination of the AFH revealed that a comparatively large BD existed in the AFH in 48%. These large BD may be a source of bile leakage when the AFHs including them are inadvertently severed during the operation. Toldt and Zuckerkandl observed, in 1875, the existence of the large BD in the AFH of a cadaveric liver by injecting Berlin blue into the common bile duct [1]. Champetier [7] and Rapant [9] also showed the dilated BDs branching off into the AFH in the figures of their article, respectively. However, it has not been clarified why comparatively large BDs so often exist in the AFH though it is an atrophied hepatic tissue. PVP is a feeding vessel of the BD developing around the intra-hepatic BDs [13–16]. As shown in Figure 4b, we noticed that the prominent PVP unexceptionally accompanied around the comparatively large BD of the AFH. This leads to conjecture that these comparatively large BDs of the AFH may be formed when the PVP persisted by chance and continued the feeding of the remnants of the BD even after the atrophy of the left liver. Our study showed that a solitary BD was hardly found in the AFH and that the BD was unexceptionally accompanied with a set of the PV and the HA. It will mean that BD heavily depends on the feeding blood vessels.

As was shown by Gao and Roberts [8], in our macroscopic findings, six types were observed in the shape of the AFH. The existence of such a variety of shapes may reflect the original shape and the degree of the atrophy in the left livers.

In conclusion, when performing dissection of the AFH, it is important to remember that the remnants of the portal tracts frequently exist in it and that these cause an unexpected bleeding or bile leakage. As indicated by Kekis [12], we also want to advise surgeons to divide the AFH not only by electrocautery but to ligate its stump securely.

Acknowledgments This study was supported by Grant-in-Aid for Scientific Research from the Ministry of Education, Science, Sports and Culture of Japan (No. 21659314, 23659636). Masako Saito, Hiroko Yamazaki, Ryuichi Aoyagi, Fujio Takahashi, Mitsuo Shikata, Yoshihiro Morimura and Masako Sin were the technicians belonging to Gunma University, Graduate School of Medicine, Maebashi, Japan. The authors are grateful to the technicians for their technical support in this study.

Conflict of interest None declared.

Author contributions Study design: Kogure and Makuuchi. Acquisition of data: Kogure, Kojima, Matsuzaki, Yorifuji and Takata. Analysis and interpretation: Kogure and Makuuchi. Drafting of the manuscript: Kogure. Revision: Makuuchi. Obtaining funding: Kogure. Administrative, technical, or material support: Matsuzaki, Yorifuji, Takata. Study supervision: Kojima, Kuwano and Makuuchi.

References

1. Toldt C, Zuckerkandl E. Über die Form- und Texturveränderungen der menschlichen Leber während des Wachsthums (in German). Sitzungsberichte der K. K. Akademie der Wissenschaften Wien. 1875;72(Abt. 3):241–95.
2. Charpy A, Soulie A. Foie. Anatomie (in French). In: Poirier P, Charpy A, editors. Traited anatomie humanie 4 (3). Paris: Masson; 1914. p. 117–203.
3. Davies DV, Coupland RE. Splanchnology. The liver. In: Davies DV, Coupland RE, editors. 34th Gray's anatomy. London and Harlow: Longmans, Green and Co Ltd; 1969. p. 1518–21.
4. Bannister LH. (Section editor). Alimentary system. Liver. In: Williams PL, Bannister LH, Berry MM, Collins P, Dyson M, Dussek J, et al., editors. 38th Gray's anatomy. The anatomical basis of medicine and surgery. Edinburgh, London, New York, Philadelphia, Sydney, Toronto: Churchill Livingstone; 1999. p. 1795–810.
5. Hobsley M. Intra-hepatic anatomy: a surgical evaluation. Br J Surg. 1958;45:635–44.
6. Foster JH, Wayson EE. Surgical significance of aberrant bile ducts. Am J Surg. 1962;104:14–19.
7. Champetier J, Davin JL, Letoublon C, Laborde Y, Yver R, Cousset F. Aberrant biliary ducts (vasa aberrantia): surgical implications. Anat Clin. 1982;4:137–45.
8. Gao XH, Roberts A. The left triangular ligament of the liver and the structures in its free edge (Appendix fibrosa hepatis) in Chinese and Canadian cadavers. Am Surg. 1986;52:246–52.
9. Rapant V, Hromada J. A contribution to the surgical significance of aberrant hepatic ducts. Ann Surg. 1950;132:253–9.
10. Iso Y, Kusaba I, Matsumata T, Okita K, Murakami N, Nozoe T, et al. Postoperative bile peritonitis caused by division of an aberrant bile duct in the left triangular ligament of the liver. Am J Gastroenterol. 1996;91:2428–30.
11. Takeuchi K, Honzumi M, Ikeda T, Hamaguchi T. A case of bile leakage from the left triangular ligament of the liver after total gastrectomy (in Japanese with English abstract). J Japan Surg Assoc. 2000;61:2715–18.
12. Kekis PB, Kordonis A, Stamou KM, Kekis BP. Surgical importance of aberrant bile ducts in the left triangular ligament of the liver. HPB. 2000;2:21–4.
13. Murakami T, Itoshima T, Shimada Y. Peribiliary portal system in the monkey liver as evidenced by the injection replica scanning electron microscope method. Arch Histol Jap. 1974;37:245–60.

14. Cho KJ, Lunderquist A. The peribiliary vascular plexus: the microvascular architecture of the bile duct in the rabbit and in clinical cases. Radiology. 1983;147:357–64.
15. Washington K, Clavien PA, Killenberg P. Peribiliary vascular plexus in primary sclerosing cholangitis and primary biliary cirrhosis. Hum Pathol. 1997;28:791–5.
16. Nakanuma Y, Hoso M, Sanzen T, Sasaki M. Microstructure and development of the normal and pathologic biliary tract in humans, including blood supply. Microsc Res Tech. 1997;38:552–70.
17. Rohen JW, Yokochi C, Lutjen-Drecoll E. Color atlas of anatomy. A photographic study of the human body. Philadelphia, Tokyo: Lippincott Williams & Wilkins; 2002. p. 286–87.
18. Couinaud C. Portal segmentation. In: Couinaud C, editor. Controlled hepatectomies and exposure of the intrahepatic bile ducts. Paris: Couinaud C; 1981. p. 9–27.
19. Engel R. Nuove ricerche sui vasi biliari aberranti (in Italian). Ric Labor Anat Norm. R. Univ. Roma, T. XV, 1911. (cited from Reference 2, p. 188–9).
20. Kogure K, Ishizki M, Nemoto M, Kuwano H, Yorifuji H, Ishikawa H, et al. Close relation between the inferior vena cava ligament and the caudate lobe in human liver. J Hepatobiliary Pancreat Surg. 2007;14:297–301.
21. Healey JE, Sterling JA. Segmental anatomy of the newborn liver. Ann N Y Acad Sci. 1963;111:25–36.
22. EL Gharbawy RM, Skandalakis LJ, Heffron TG, Skandalakis JE. Aberrant bile ducts, "Remnant surface bile ducts," and peribiliary glands: descriptive anatomy, historical nomenclature, and surgical implications. Clin Anat. 2011;24:429–40.
23. Missen AJB. Aberrations of the biliary passages on the surface of the liver and gall-bladder and in the gall-bladder wall. Br J Surg. 1969;56:427–31.
24. Collins P. Embryology and development. In: Williams PL, Bannister LH, Berry MM, Collins P, Dyson M, Dussek J, et al., editors. 38th Gray's anatomy. The anatomical basis of medicine and surgery. Edinburgh, London, New York, Philadelphia, Sydney, Toronto: Churchill Livingstone; 1999. p. 187–8.
25. Healey JE, Schroy PC. Anatomy of the biliary ducts within the human liver. Analysis of prevailing pattern of branchings and the major variations of the biliary ducts. Arch Surg. 1953;66:599–644.

World Journal of Gastroenterology

Submit a Manuscript: http://www.wjgnet.com/esps/
Help Desk: http://www.wjgnet.com/esps/helpdesk.aspx
DOI: 10.3748/wjg.v20.i42.15691

World J Gastroenterol 2014 November 14; 20(42): 15691-15702
ISSN 1007-9327 (print) ISSN 2219-2840 (online)

ORIGINAL ARTICLE

Mechanism of gastrointestinal abnormal motor activity induced by cisplatin in conscious dogs

Hiroyuki Ando, Erito Mochiki, Tetsuro Ohno, Mitsuhiro Yanai, Yoshitaka Toyomasu, Kyoichi Ogata, Yuichi Tabe, Ryuusuke Aihara, Toshihiro Nakabayashi, Takayuki Asao, Hiroyuki Kuwano

Hiroyuki Ando, Erito Mochiki, Tetsuro Ohno, Mitsuhiro Yanai, Yoshitaka Toyomasu, Kyoichi Ogata, Yuichi Tabe, Ryuusuke Aihara, Toshihiro Nakabayashi, Takayuki Asao, Hiroyuki Kuwano, Department of General Surgical Science, Gunma University Graduate School of Medicine, Gunma 371-8511, Japan

Author contributions: Ando H and Mochiki E contributed equally to this work; Ando H, Mochiki E, Ohno T, Yanai M, Toyomasu Y, Ogata K, Tabe Y, Aihara R, Nakabayashi T, Asao T and Kuwano H designed the research; Ando H, Ohno T, Yanai M, Toyomasu Y, Ogata K and Tabe Y performed the research; Ando H, Ohno T, Nakabayashi T and Asao T contributed new reagents/analytic tools; Ando H, Mochiki E, Ohno T, Aihara R, Asao T and Kuwano H analyzed the data; Ando H, Mochiki E and Kuwano H wrote the paper.

Correspondence to: Hiroyuki Ando, MD, PhD, Department of General Surgical Science, Gunma University Graduate School of Medicine, 3-39-22 Showa-machi, Maebashi, Gunma 371-8511, Japan. andu07120404andu@yahoo.co.jp
Telephone: +81-27-2208224 Fax: +81-27-2208230
Received: February 22, 2014 Revised: March 25, 2014
Accepted: June 2, 2014
Published online: November 14, 2014

Abstract

AIM: To investigate whether 5-hydroxytryptamine (serotonin; 5-HT) is involved in mediating abnormal motor activity in dogs after cisplatin administration.

METHODS: After the dogs had been given a 2-wk recovery period, all of them were administered cisplatin, and the motor activity was recorded using strain gauge force transducers. Blood and intestinal fluid samples were collected to measure 5-HT for 24 h. To determine whether 5-HT in plasma or that in intestinal fluids is more closely related to abnormal motor activity we injected 5-HT into the bloodstream and the intestinal tract of the dogs.

RESULTS: Cisplatin given intravenously produced abnormal motor activity that lasted up to 5 h. From 3 to 4 h after cisplatin administration, normal intact dogs exhibited retropropagation of motor activity accompanied by emesis. The concentration of 5-HT in plasma reached the peak at 4 h, and that in intestinal fluids reached the peak at 3 h. In normal intact dogs with resection of the vagus nerve that were administered kytril, cisplatin given intravenously did not produce abnormal motor activity. Intestinal serotonin administration did not produce abnormal motor activity, but intravenous serotonin administration did.

CONCLUSION: After the intravenous administration of cisplatin, abnormal motor activity was produced in the involved vagus nerve and in the involved serotonergic neurons *via* another pathway. This study was the first to determine the relationship between 5-HT and emesis-induced motor activity.

Key words: Cisplatin; Emesis; 5-hydroxytryptamine; Abnormal motor activity; Dog

Core tip: Previous studies have investigated the motility change unique to cisplatin-induced emesis. This study is the first to investigate whether 5-hydroxytryptamine (serotonin; 5-HT) is involved in mediating abnormal motor activity in dogs after cisplatin administration. Cisplatin given intravenously produced abnormal motor activity that lasted up to 5 h. In normal dogs with resection of the vagus nerve that were administered 5-HT 3 receptor antagonist (kytril), cisplatin given intravenously did not produce abnormal motor activity. Abnormal motor activity was produced in the involved vagus nerve and in the involved serotonergic neurons *via* another pathway.

Ando H, Mochiki E, Ohno T, Yanai M, Toyomasu Y, Ogata K, Tabe Y, Aihara R, Nakabayashi T, Asao T, Kuwano H. Mechanism of gastrointestinal abnormal motor activity induced by cisplatin in conscious dogs. *World J Gastroenterol* 2014; 20(42): 15691-15702 Available from: URL: http://www.wjgnet.com/1007-9327/full/v20/i42/15691.htm DOI: http://dx.doi.org/10.3748/wjg.v20.i42.15691

INTRODUCTION

Cisplatin is a widely used chemotherapeutic drug in cancer treatment; however, it produces many side effects, including nephrotoxicity, emesis, and diarrhea[1]. Emesis is an especially common and severe side effect after cisplatin administration. The main mechanism of cancer chemotherapeutic induced acute emesis is thought to be the stimulation of the vomiting center of the medulla oblongata by 5-hydroxytryptamine (serotonin; 5-HT), which is released from intestinal enterochromaffin (EC) cells following cisplatin administration *via* afferent vagal nerve fibers[2]. Suppression of nausea appears to be due to an antagonistic action on the 5-HT3 receptors[3]. After the 5-HT receptors were classified by Bradley *et al*[4], selective antagonists of 5-HT3 receptors were developed. Many studies have confirmed the pharmacological role of 5-HT, and particularly 5-HT3 receptors, in the control of anticancer drug-induced emesis[5]. However, the mechanism of emesis-induced abnormal gastrointestinal motility remains unclear.

The gastrointestinal (GI) tract is the largest single store of 5-HT within the mammalian body due to the presence of EC cells in the intestinal mucosa[6] and serotonergic neurons in the enteric nervous system, such as the myenteric plexus[7]. Most of the experiments have been carried out *in vitro*[8-10]. One study has shown that 5-HT can be released from EC cells into the intestinal lumen[11] and portal circulation *via* mechanisms associated with cholinergic and adrenergic actions, intraluminal pressure, hypertonic glucose, or luminal acidification[10,12]. However, the precise role of 5-HT in the occurrence of vomiting has not been fully elucidated.

Since emesis is known to be accompanied by abnormal gastrointestinal motility[13-17], in the present study, we focused on both gastrointestinal motor activity and the concentrations of 5-HT in plasma and intestinal fluids of conscious dogs after intravenous administration of cisplatin. We investigated whether 5-HT is involved in mediating abnormal gastrointestinal motor activity in conscious dogs. We also studied the relationship between plasma and luminal concentrations of 5-HT in conscious dogs after intravenous administration of cisplatin. This study is the first to determine the relationship between 5-HT and emesis-induced gastrointestinal motor activity.

MATERIALS AND METHODS

Animal preparation

Healthy mongrel dogs of both sexes weighing 10-15 kg were used. All dogs were fasted overnight and then anesthetized by a single intravenous injection of thiopental sodium (Ravonal; Tanabe Pharmaceutical, Osaka, Japan; 20 mg/kg body weight). General anesthesia was maintained by intratracheal inhalation of halothane (Fluothane; Takeda Chemical Industries, Osaka, Japan) and oxygen. A silastic tube (Silastic 602-205; Dow Corning, Midland, MI) was inserted into the superior vena cava through a branch of the right external jugular vein (jugular tube) and used for the withdrawal of blood samples and injections. The jugular tube was brought out through a skin incision on the neck, and its outer end was fixed to the adjacent skin with silk sutures. The abdominal cavity was opened by a middle incision.

Force transducers were implanted on the serosal surfaces of the gastric body, antrum, pylorus, mid-duodenum, and jejunum 1 and 2 (20 and 40 cm distal to Treitz's ligament, respectively). Another silastic tube (Silicone tube SR1554; Tigers Polymer, Osaka, Japan) was inserted into the duodenum through the duodenal wall (duodenal tube) and used for the injection of agents and the withdrawal of intestinal fluid samples. The lead wires of the force transducers and the duodenal tube were taken out of the abdominal cavity through a subcutaneous tunnel and brought out through a skin incision made between the right and left scapula. After closure of the abdominal cavity, a jacket-type protector was placed on each dog to protect the lead wires and tubes from being damaged if the dogs scratched themselves. The dogs were housed in individual experiment cages, maintained with intravenous drip infusions of Lactec G (Otsuka Pharmaceutical, Tokyo, Japan) for 6 d postoperatively, and gradually returned to normal dog food (Funabashi Farm, Funabashi, Japan; 15 g/kg body weight per day). This study was approved by the Review Committee on Animal Use at Gunma University, Maebashi, Japan (07-139).

Monitoring of gastrointestinal contractions

The wires from the transducer were connected to a telemeter, and the data were transmitted to a recording system (Eight Star system, Star Medical, Tokyo, Japan). Recorded signals were used to determine the motility index (MI) values. The MI was the integrated area between the baseline (zero level) and the contractile wave expressed as motor units measured with the Eight Star system. In addition, the data were used to identify the phases of contractile activity. Each phase was visually determined according to the following criteria: the quiescent period was defined as phase I; phase II consisted of clusters of irregular contractions that followed phase I and preceded phase III; phase III was the period during which a

group of strong contractions lasting more than 15 min occurred; and phase Ⅳ was a short period of subsiding contractions immediately following the phase Ⅲ contractions.

Test substances

Cisplatin and 5-HT (serotonin hydrochloride: Sigma-Aldrich Japan K.K., Tokyo, Japan) were dissolved in an injection solvent (Hikari Pharmaceutical, Tokyo, Japan) immediately before use. Cisplatin was donated by Nippon Kayaku (Tokyo, Japan). The dexamethasone sodium phosphate (decadron phosphate injection; Banyu Pharmaceutical, Tokyo, Japan), α-receptor antagonist phentolamine (regitin) (Novartis Pharma K.K., Tokyo, Japan), β-receptor antagonist propranolol (inderal) (AstraZeneca K.K., Osaka, Japan), 5-HT3 receptor antagonist (kytril) (Chugai Pharmaceutical, Tokyo, Japan), muscarinic receptor antagonist atropine (Tanabe Pharmaceutical, Osaka, Japan), and dopamine D_2 receptor antagonist (prinperan) (Astellas Pharmaceutical, Tokyo, Japan) were purchased. The antagonist doses were determined according to previous studies[2,10,18-22]. Emesis did not occur in dogs receiving 1.0 mg/kg cisplatin; however, it did occur in dogs receiving 1.2 mg/kg cisplatin, which was the dose selected for the present study. In previous studies[19,20,22], dogs were usually given cisplatin at a dose of 3.0 mg/kg, about three times higher than the dose administered in the present low-dose study. Before each intravenous administration of cisplatin, we confirmed that there was no abnormal motor activity.

Experimental protocol

Effects of cisplatin and drugs on cisplatin-induced emesis: The experiments were started after all the dogs had been given a 2-wk recovery period. Before cisplatin administration, the interdigestive state of each dog was recorded for at least 6 h as a control study. After control data were obtained from each dog, the study with cisplatin and various other drugs commenced. After the interdigestive migrating motor contractions (IMCs) were confirmed to have occurred and 20 min after the spontaneous phase Ⅲ contractions of the jejunum 2 (40 cm distal to Treitz's ligament) had terminated, all the dogs were administered cisplatin (1.2 mg/kg). Blood and intestinal fluid samples were withdrawn from the jugular tube and duodenal tube 0, 1, 3, 4, 5, 7, 9, and 24 h later, and 5-HT was measured. For the 5-HT measurements, whole blood and intestinal fluids were collected in vacuum plastic tubes containing ethylenediaminetetraacetic acid (EDTA) 2Na. The fluids were then frozen and stored at -30 ℃ until assaying. The samples were subjected to high-performance liquid chromatography (HPLC) (BMT., Kawagoe, Japan).

Dexamethasone (1 mg/kg), phentolamine (regitin; 0.5 mg/kg), propranolol (inderal; 0.5 mg/kg), or granisetron (kytril; 0.05 mg/kg) was given as a single-bolus injection 20 min after the spontaneous phase Ⅲ contractions of the jejunum 2 had terminated. Granisetron (kytril; 0.05 mg/kg) was also given as a single-bolus injection in the dogs. Cisplatin (1.2 mg/kg) was given 1 h after the administration of each inhibitor.

Atropine (0.05 mg/kg + 0.05 mg/kg per hour) was given as a single-bolus injection. The injection was followed by a 30-min continuous intravenous infusion starting 20 min after the spontaneous phase Ⅲ contractions of the jejunum 2 had terminated. Metoclopramide (0.5 mg/kg + 0.5 mg/kg per hour) was given as a single-bolus injection. This injection was followed by a 5-h continuous intravenous infusion starting 20 min after the spontaneous phase Ⅲ contractions of the jejunum 2 had terminated. Cisplatin (1.2 mg/kg) was given 1 h after the start of the administration of each inhibitor.

Then, the dogs were divided into two groups: a normal intact dog group (ND) and a normal intact dog group with resection of the vagus nerve (NDRVN). The NDRVN (n = 4) underwent a truncal vagotomy, with the ventral and dorsal vagi cut immediately below the diaphragm. The dogs in the ND (n = 10) did not undergo surgery and served as the control group.

Effect of 5-HT

After the IMCs were confirmed to have occurred and 20 min after the spontaneous phase Ⅲ contractions of the jejunum 2 had terminated, the ND and NDRVN were administered 5-HT intravenously through the jugular tube (600 μg/kg) and into the duodenum through the duodenal tube (600 and 5400 μg/kg) according to the procedures described in previous studies[2,10,18-22]. Zhu *et al*[10] reported that intraluminal infusion of 10^{-5} M 5-HT elicited increases in vagal afferent discharge by activating the 5-HT3 receptors in rats. Following the procedures described previously[10], we administered 5-HT (200 μg/kg) according to the conversion of the mol concentration. In the dogs, such doses of an intraluminal infusion of 5-HT did not elicit abnormal motor activity, but three-fold doses (600 μg/kg) did. The subsequent gastrointestinal motility was recorded for at least 4 h. The MI values during the 60 min following 5-HT administration (600 μg/kg) were calculated for the ND and NDRVN.

Analysis of data

Gastrointestinal motility was quantified by calculating the MI, which was equivalent to the area under the curve. The MI was calculated using a computer-assisted system (Eight Star system, version 6.0, Star Medical, Tokyo, Japan). Gastrointestinal motility after 5-HT administration (600 μg/kg) was analyzed for 60 min.

Statistical analysis

Results are expressed as mean ± SE. The data were subjected to detailed statistical analyses using repeated measures of analysis of variance (ANOVA). When significant differences were detected, differences between means were checked using the Fisher's protected least significant difference test. The Mann-Whitney U test was used to test the significance of differences among groups. P-val-

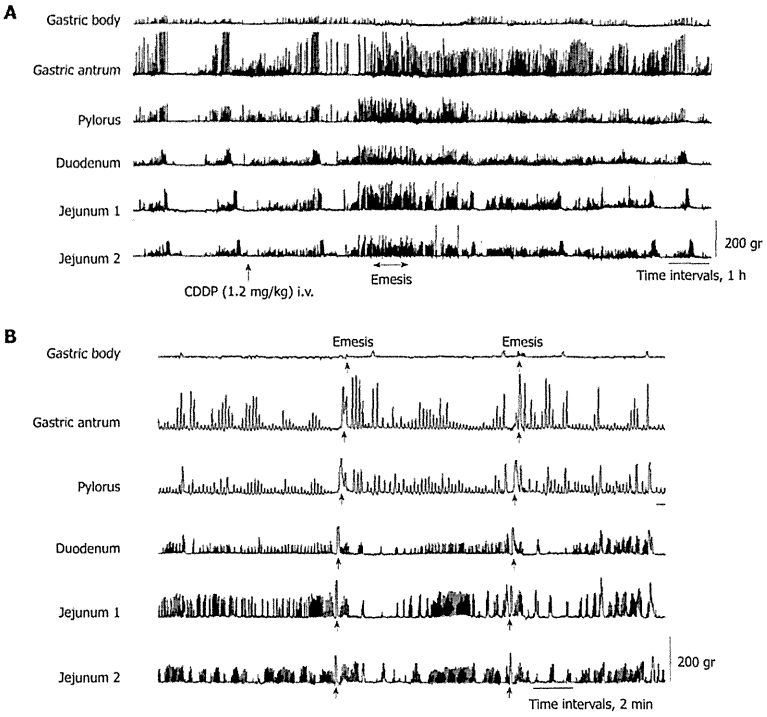

Figure 1 Interdigestive motor activity observed after intravenous administration of cisplatin (1.2 mg/kg). A: Interdigestive motor activity was observed in the ND (n = 10); B: From approximately 3 to 4 h after the intravenous administration of cisplatin, the ND exhibited retropropagation of gastrointestinal motor activity from jejunum 2 to the gastric body, accompanied by emesis. ND: Normal intact dog group; i.v.: Intravenous administration.

ues < 0.05 were considered significant. Statistical calculations were performed with the use of StatView® software (version 5.0; Abacus Concepts, Inc., Berkeley, CA).

RESULTS

Effects of cisplatin on gastrointestinal contractions and cyclic 5-HT concentrations in plasma and intestinal fluids

In all dogs in the fasted state, cyclic changes of contractions were detected, including a quiescence period followed by a group of strong contractions (phase III). Abnormal motor activity in the dogs developed from the duodenum, followed by jejunum 1 and 2 and the antrum and pylorus about 2.5 h after intravenous administration of cisplatin (Figure 1A). Cisplatin given intravenously resulted in the complete interruption of IMCs and predominantly produced abnormal motor activity which lasted up to 5 h (Figure 1A). From about 3 to 4 h after the intravenous administration of cisplatin, the dogs exhibited retropropagation of gastrointestinal motor contractions from jejunum 2 to the gastric body, accompanied by emesis (Figure 1B). The most frequent emetic episodes were observed from 3 to 4 h after cisplatin administration. Emesis developed in all the dogs.

The concentrations of 5-HT in plasma and intestinal fluids determined in these experiments are shown in Figure 2. The plasma 5-HT concentration increased, reached the peak at 4 h after the intravenous administration of cisplatin, and then exhibited small fluctuations and declined (Figure 2A). The plasma 5-HT concentration at 0 h was significantly higher than those obtained at 4 and 7 h ($P < 0.05$). The 5-HT concentrations in intestinal fluids increased, reached the peak at 3 h after the intravenous administration of cisplatin, and then declined (Figure 2B). The 5-HT concentration in intestinal fluids at 0 h was significantly higher than those obtained at 3, 4, and 5 h ($P < 0.05$).

Effects of drugs and vagotomy on cisplatin-induced abnormal motor activity

After dexamethasone (1 mg/kg), phentolamine (regitin; 0.5 mg/kg), propranolol (inderal; 0.5 mg/kg), atropine (0.05 mg/kg + 0.05 mg/kg per hour), or metoclo-

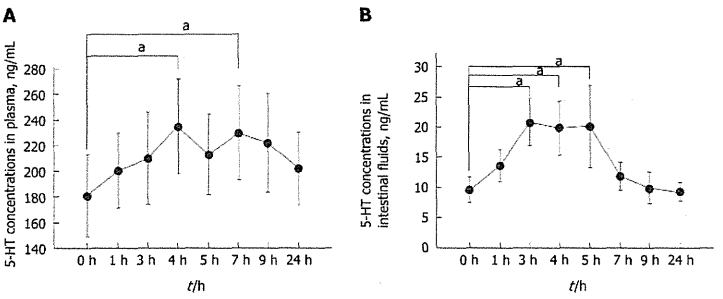

Figure 2 Changes in concentrations of 5-hydroxytryptamine in plasma and intestinal fluids. A: Changes in the plasma 5-HT concentrations in ND (n = 10). Each symbol represents mean ± SE. The plasma 5-HT concentration obtained at 0 h was significantly higher than those obtained at 4 and 7 h ($^aP < 0.05$); B: Changes in the 5-HT concentrations in intestinal fluids in ND (n = 10). Each symbol represents mean ± SE. The 5-HT concentration in intestinal fluids at 0 h was significantly higher than those obtained at 3, 4, and 5 h ($^aP < 0.05$). 5-HT: 5-hydroxytryptamine; ND: Normal intact dog group.

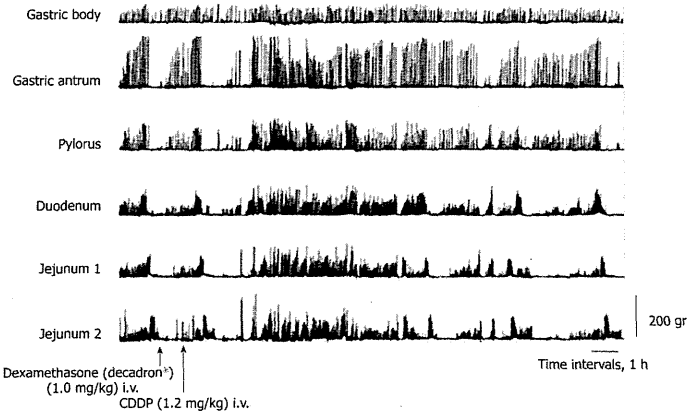

Figure 3 In normal intact dog group, cisplatin (1.2 mg/kg) was given 1 h after dexamethasone administration (1.0 mg/kg), and interdigestive motor activity was observed.

pramide (0.5 mg/kg + 0.5 mg/kg per hour) administration, cisplatin given intravenously also resulted in the complete interruption of IMCs and predominantly produced abnormal motor activity that lasted up to about 5 h (Figures 3 and 4). However, in dogs that had received intravenous metoclopramide, emesis did not occur. In the NDRVN (n = 4) (Figure 5A), cisplatin given intravenously also produced abnormal motor activity that, however, lasted for a shorter duration. After the NDRVN (n = 4) was administered granisetron (kytril; 0.05 mg/kg), cisplatin given intravenously did not produce abnormal motor activity (Figure 5B). In the ND (n = 6) administered granisetron (kytril; 0.05 mg/kg) (Figure 6), cisplatin given intravenously also produced abnormal motor activity that, however, lasted for a shorter duration. In three of the four NDRVN dogs and three of the six ND dogs that received granisetron (kytril; 0.05 mg/kg), emesis did not occur. The emetic episodes in the dogs receiving cisplatin alone (control, n = 10), granisetron (kytril; 0.05 mg/kg, i.v., n = 6), and NDRVN dogs (n = 4) are shown in Figure 7. The emetic episodes were, respectively, 5.80 ± 0.66, 0.66 ± 0.33, and 0.25 ± 0.25 in the control group, granisetron (kytril) group, and NDRVN. Significant differences were detected among the control group, kytril group, and NDRVN ($P < 0.05$).

Effect of 5-HT

To determine whether 5-HT in plasma or in intestinal fluids causes abnormal motor activity, we administered 5-HT intravenously through the jugular tube (600 μg/kg) (Figures 8A and 9A) and into the duodenum through the duodenal tube (600 and 5400 μg/kg) (Figures 8B, 9B, and C), respectively, in the ND and NDRVN.

In the ND, after the intravenous administration of

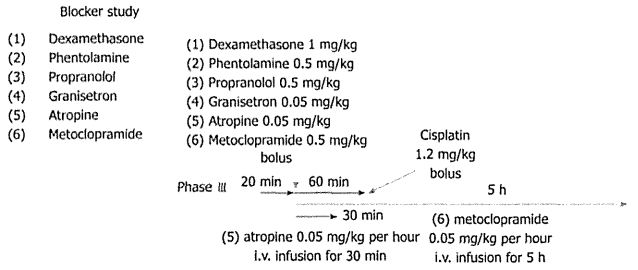

Figure 4 Blocker study chart. In the ND, dexamethasone (1 mg/kg), phentolamine (regitin; 0.5 mg/kg), propranolol (inderal; 0.5 mg/kg), or granisetron (kytril; 0.05 mg/kg) was given as a single-bolus injection starting 20 min after the spontaneous phase III contractions of the jejunum 2 had terminated. Kytril (0.05 mg/kg) was also given as a single-bolus injection in the ND and NDRVN (n = 4). Cisplatin (1.2 mg/kg) was given 1 h after the administration of each inhibitor. In ND, atropine (0.05 mg/kg + 0.05 mg/kg per hour) was given as a single-bolus injection, followed by a 30-min continuous intravenous infusion starting 20 min after the spontaneous phase III contractions of the jejunum 2 had terminated. In the ND, metoclopramide (0.5 mg/kg + 0.5 mg/kg per hour) was given as a single-bolus injection, followed by a 5-h continuous intravenous infusion starting 20 min after the spontaneous phase III contractions of the jejunum 2 had terminated. Cisplatin (1.2 mg/kg) was given 1 h after the start of the administration of each inhibitor. ND: Normal intact dog group; NDRVN: Normal intact dog group with resection of the vagus nerve; i.v.: Intravenous administration.

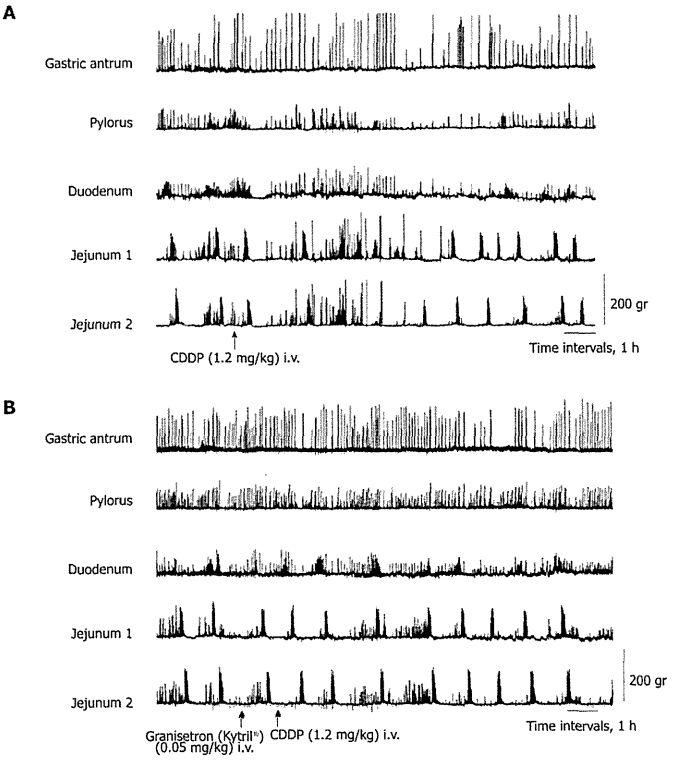

Figure 5 In normal intact dog group with resection of the vagus nerve, interdigestive motor activity was observed after the intravenous administration of cisplatin (1.2 mg/kg). A: Normal intact dog group with resection of the vagus nerve (NDRVN) (n = 4) was given cisplatin (1.2 mg/kg), and interdigestive motor activity was observed; B: In the NDRVN (n = 4), cisplatin (1.2 mg/kg) was given 1 h after granisetron (kytril) administration (0.05 mg/kg), and interdigestive motor activity was observed. i.v.: Intravenous administration.

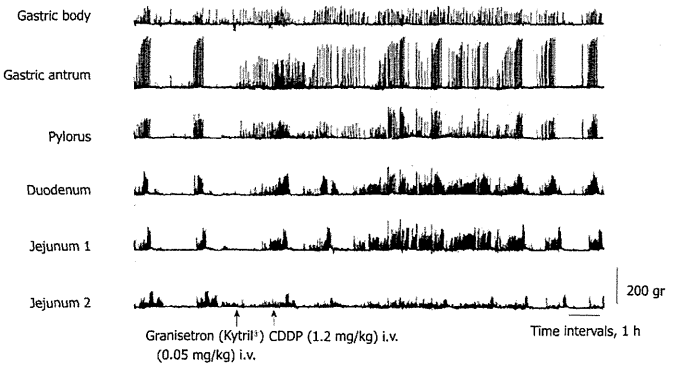

Figure 6 In the normal intact dog group (n = 6), cisplatin (1.2 mg/kg) was given 1 h after granisetron (kytril) administration (0.05 mg/kg), and interdigestive motor activity was observed.

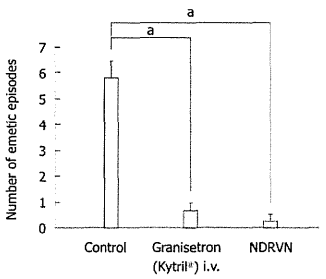

Figure 7 Numbers of emetic episodes in dogs receiving cisplatin alone (control, n = 10), kytril (0.05 mg/kg, intravenous administration, n = 6) alone, and vagotomy (the normal intact dog group with resection of the vagus nerve; n = 4). Each bar represents mean ± SE. Significant differences were detected among the control group, granisetron (kytril) group, and normal intact dog group with resection of the vagus nerve (NDRVN). Control, open bar; i.v., hatched line; RNG, filled bar. $^aP < 0.05$ *vs* control. i.v.: Intravenous administration.

5-HT (600 μg/kg), phasic contractions, such as abnormal motor activity lasting for about 30 min, were induced immediately in the antrum, pylorus, duodenum, and jejunum 1 and 2. The duration and amplitude of the motor activity in the antrum and pylorus were longer and stronger than those in the duodenum and jejunum (Figure 8A). In the NDRVN, after the intravenous administration of 5-HT (600 μg/kg), phasic contractions, such as abnormal motor activity lasting for 10 to 20 min, were immediately induced in the pylorus, duodenum, and jejunum 1 and 2. The duration and amplitude of motor activity were not longer or stronger than those in the ND (Figure 9A). In the ND and NDRVN, after the intraduodenal administration of 5-HT (600 μg/kg), phasic contractions, such as abnormal motor activity lasting for about 10 min, were immediately induced in the duodenum and jejunum 1 and 2 (Figures 8B and 9B). In the ND and NDRVN, contractions induced by the intraduodenal administration of 5-HT were obviously shorter and weaker than those resulting from intravenous administration. In the NDRVN, the duration and amplitude tended to increase as the dose of 5-HT was increased, and after the intraduodenal administration of 5-HT (5400 μg/kg), phasic contractions, such as phase Ⅱ-like activity lasting for about 1 h, were immediately induced in the pylorus, duodenum, and jejunum 1 and 2 (Figure 9C). The pattern of these contractions induced by the intravenous administration of 5-HT was different from that of spontaneously occurring IMCs.

MI data were recorded for 60 min after the intravenous and intraduodenal administration of 5-HT (600 μg/kg) in the ND (n = 4) (Figure 10A) and the NDRVN (n = 4) (Figure 10B). The MI for the intravenous administration was higher than that for the intraduodenal administration in the antrum, duodenum, jejunum 1, and jejunum 2. In the MI of the antrum, duodenum, jejunum 1, and jejunum 2 in the ND showed significant differences between the intravenous and intraduodenal groups ($P < 0.05$) (Figure 10A).

DISCUSSION

In this study, when cisplatin was given intravenously, IMCs disappeared and were replaced predominantly by abnormal phase Ⅱ-like motor activity. Thus, in all dogs, phase Ⅰ, Ⅲ, and Ⅳ activities either disappeared or markedly decreased in duration, and abnormal motor activity developed for about 5 h, starting at 2.5 h after cisplatin administration. Retropropagation of gastrointestinal motor activity originating from jejunum 2 occurred in all dogs in which emesis developed. This motility change, unique to emesis, was similar to that reported in other studies[14-17]. The present study is the first to characterize and quantify gastrointestinal motor responses during cisplatin administration.

When the concentrations of 5-HT in plasma and intestinal fluids increased, IMCs disappeared and were

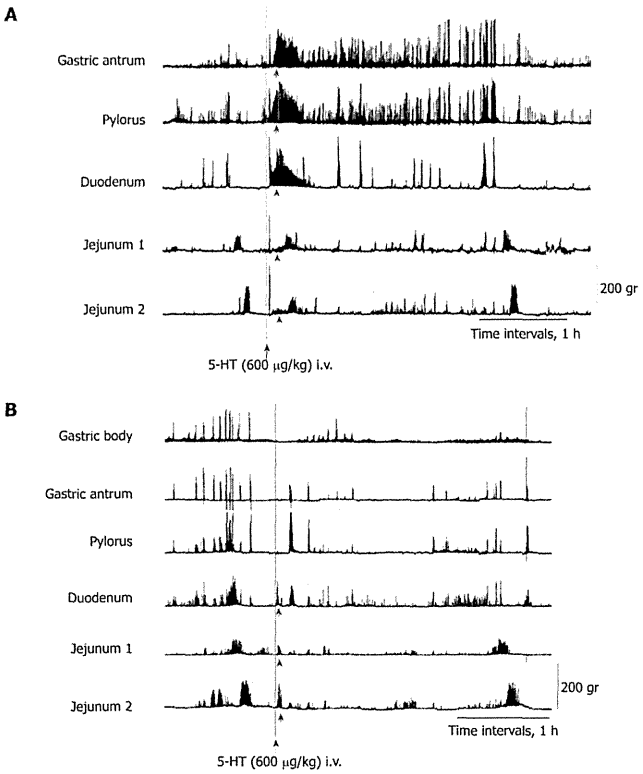

Figure 8 Responses to the intravenous and duodenal administration of 5-hydroxytryptamine in the normal intact dog group. A: Responses to the intravenous administration of 5-hydroxytryptamine (5-HT) (600 μg/kg) in the ND; B: Responses to the duodenal administration of 5-HT (600 μg/kg) in the ND. ND: Normal intact dog group; i.v.: Intravenous administration; i.d.: Intraduodenal administration.

replaced predominantly by abnormal motor activity. To determine whether 5-HT in plasma or in intestinal fluids is more closely related to abnormal motor activity, we administered 5-HT into the vein and the intestinal tract of the dogs. Motor activity similar to cisplatin-induced abnormal motor activity was produced by intravenous serotonin administration. We administered the same amount of serotonin into the duodenum, but the reaction was negligible. The dose of intravenously administered serotonin was different from the maximal value of 5-HT, which we measured after cisplatin administration. We did not measure the 5-HT concentration in whole blood but in plasma because the platelets, which are in whole blood, include the most 5-HT. We assumed that the doses of intravenously administrated serotonin were different from the maximal value of 5-HT measured after cisplatin administration.

Most of the 5-HT from EC cells is secreted *via* the basolateral membrane into the portal circulation; a smaller portion is released from the apical membrane into the intestinal lumen[23]. The basal vascular release of serotonin was 10 times higher than the luminal release[24]. Serotonin released from the basolateral site of the EC cells may reach the connective tissue space of the lamina propria and exert paracrine effects on either endocrine cells or intrinsic and extrinsic nerve terminals[24]. It has been reported that exogenously applied serotonin inhibits acid secretion and that this effect is exerted by serotonin injected into blood vessels but not by serotonin injected into the gastric lumen[25]. Judging from the previous results, serotonin released from the basolateral site of the EC cells seems to be more important than serotonin released from the apical site of the EC cells. Our results are in good agreement with those of previous studies, confirming that abnormal motor activity is produced by intravenous serotonin administration.

We investigated the effects of various antagonists on abnormal activity induced by cisplatin administration. Cisplatin-induced responses, which are abnormal activities, were not inhibited by dexamethasone, phentolamine,